

# CrystEngComm

Accepted Manuscript



This is an *Accepted Manuscript*, which has been through the Royal Society of Chemistry peer review process and has been accepted for publication.

*Accepted Manuscripts* are published online shortly after acceptance, before technical editing, formatting and proof reading. Using this free service, authors can make their results available to the community, in citable form, before we publish the edited article. We will replace this *Accepted Manuscript* with the edited and formatted *Advance Article* as soon as it is available.

You can find more information about *Accepted Manuscripts* in the [Information for Authors](#).

Please note that technical editing may introduce minor changes to the text and/or graphics, which may alter content. The journal's standard [Terms & Conditions](#) and the [Ethical guidelines](#) still apply. In no event shall the Royal Society of Chemistry be held responsible for any errors or omissions in this *Accepted Manuscript* or any consequences arising from the use of any information it contains.

# Thermodynamics and crystallization of the theophylline – salicylic acid cocrystal

Cite this: DOI: 10.1039/x0xx00000x

S. Zhang,<sup>a</sup> H. Chen<sup>c,d</sup> and Å. C. Rasmuson<sup>a,b</sup>

Received 00th January 2012,  
Accepted 00th January 2012

DOI: 10.1039/x0xx00000x

www.rsc.org/

The 1:1 theophylline – salicylic acid cocrystals has been successfully prepared by slurry conversion crystallization in a 1:1 mole ratio slurry of theophylline and salicylic acid in chloroform. The cocrystal powder has been analysed by XRD and DSC, and the cocrystal structure has been determined by single crystal XRD. The cocrystal melts at 188.5 °C, in-between the melting points of the pure cocrystal components. Microscope and SEM images have been taken for the cocrystals prepared by slow evaporation from ethanol, ethyl acetate, or acetonitrile. The cocrystal dissolves congruently in chloroform and the solubility has been determined. Based on the solubility data of the cocrystal and of the pure components, the Gibbs free energy of the cocrystal formation is calculated to be -4.92 kJ/mol at 30 °C. The cocrystal dissolves incongruently in methanol, ethanol, and acetonitrile. The ternary phase diagram of the cocrystal in acetonitrile has been determined, and is compared with those of the theophylline – oxalic acid cocrystal and theophylline – glutaric acid cocrystal systems. By proper allocation of the process in the phase diagram, the theophylline – salicylic acid cocrystal can be produced by slurry conversion crystallization in acetonitrile.

## Introduction

Formation of cocrystal of active pharmaceutical ingredients (API) gives additional opportunities for fine-tuning physical properties of the drug like stability, hygroscopicity, melting point, and solubility. The cocrystal of caffeine and theophylline has improved resistance to hydration,<sup>1-4</sup> and other reports reveal cocrystals with good resistance to degradation.<sup>5-7</sup> In a survey of 50 pharmaceutical cocrystals, it is shown that approximately half of them have a melting point in between those of the two cocrystal components.<sup>8</sup> Among several cocrystals of 4,4'-bipyridine, those with molecules packing in a herringbone arrangement obtain higher melting point than those with channel structure.<sup>9</sup> A study of n-alkyl carboxylic acid – pyrazine cocrystal shows that the cocrystal structures display regularity for acids longer than C7 (heptanoic acid and longer), and the cocrystals show an alternation in their melting point which is opposite to that in the n-alkyl carboxylic acid themselves.<sup>10</sup> Thus the relation between the melting point and cocrystal structure is worth being analysed for the rational design of new cocrystals in the future.

In recent modelling and experimental work,<sup>11-13</sup> it has been shown that the cocrystal phase diagram exhibits a systematic dependence on the solubility of the cocrystal components. The larger the solubility difference between the pure cocrystal components, the more likely it is that the cocrystal dissolves incongruently – i.e. the cocrystal is not stable in the corresponding stoichiometric solution but the stability region of the cocrystal<sup>12,13</sup> is shifted outside of the stoichiometry line.

Based on the determination of the ternary phase diagram, the thermodynamic and kinetic aspects of a cocrystallization process and scale-up issues have been discussed in several reports.<sup>14-19</sup> With the knowledge of the phase diagram, the cocrystal can be prepared in industrial scale also for incongruently dissolving systems.<sup>12</sup> Therefore, as a crucial aspect of cocrystal investigations, a systematic study of the phase diagrams of a series of cocrystals of the same drug molecule may be needed and helpful to understand the alternatives for manufacturing.

In this work, the thermodynamics and crystallization behaviour of the theophylline – salicylic acid cocrystal is studied, and compared with the properties of theophylline – oxalic acid and theophylline – glutaric acid cocrystals. Theophylline is a typical purine derivative, which is used for asthma therapy and as a diuretic. It has both good hydrogen bond acceptors and donors, and is known to form a few polymorphs and a monohydrate,<sup>20-28</sup> and has been reported to form cocrystals with several carboxylic acids.<sup>1</sup> Salicylic acid is the ortho form of monohydroxybenzoic acid. Since ancient times, it is known for the ability of pain and fever relief. Now it is best known for the use in anti-acne treatments. No polymorphs of salicylic acid have been reported so far. Similar to other carboxylic acids, the –COOH group makes it a good cocrystal cofomer to theophylline. The chemical structures of the molecules in this work are shown in Figure 1.

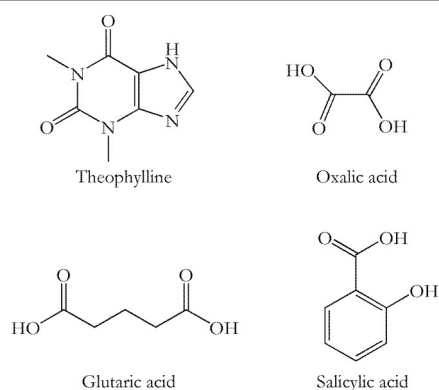


Figure 1 Chemical structure of theophylline, salicylic acid, and other cocrystal cofomers.

## Experimental work

### Materials

Salicylic acid (99%) and Theophylline (anhydrous, >99%) (Form II)<sup>29</sup> were purchased from Sigma-Aldrich. Acetonitrile (>99.8%), ethyl acetate (for HPLC, >99.8%) and chloroform (for HPLC, >99.9%) were purchased from VWR/Merck. Ethanol (E, purity >99.7%) was from Solveco. All the chemicals were used as received.

### Preparation of cocrystal

Batches of the theophylline – salicylic acid cocrystal were prepared in 250 ml glass bottles with magnetic stir bars by isothermal slurry conversion of a stoichiometric 1 : 1 molar ratio mixture of solid theophylline and solid salicylic acid in chloroform. The cocrystals for single crystal XRD and SEM imaging were prepared by slow evaporation from a 1 : 1 stoichiometric chloroform solution seeded or non-seeded.

### Solid phase characterisation

A TA Instruments DSC2920 was calibrated with indium according to the standard procedure and was used to collect the differential scanning calorimetry (DSC) data by using a 5 °C min<sup>-1</sup> ramp rate from room temperature to 300 °C. X ray diffraction (XRD) powder data were collected by a PANalytical XPert Pro powder diffractometer with Cu K $\alpha$  radiation. Scanning electron microscopy (SEM) images of the cocrystal were captured by a Hitachi SU – 70. A Cary 300 Bio UV-vis/Varian was used in the ternary phase diagram determination. Single crystal X-ray diffraction data for structure determination was collected at 180 K on an supernova, Atlas diffractometer, with Cu K $\alpha$ 1 radiation ( $\lambda = 1.54056 \text{ \AA}$ ). Further data were collected by the same apparatus for determination of how the unit cell changes with temperature. Data integration and multi-scan absorption correction were carried out by the CrysAlis software package from Oxford Diffraction.<sup>30</sup> Structure was solved by the direct method. Non-hydrogen atoms were located directly from difference Fourier maps. Final structure refinements were performed with the SHELX program by

minimizing the sum of the squared deviation of  $F^2$  using a full matrix technique.<sup>31</sup>

The Gibbs free energy of the cocrystal formation was estimated using the solubility data. The enthalpy of formation of the cocrystal was estimated from DSC data,<sup>32,33</sup> integrating heat flow data from the melting point and subtracting the data for the physical mixture of the two solid components from that of the cocrystal.

### Solid-liquid solubility and Phase diagram determination

The theophylline – salicylic acid cocrystal dissolves congruently in chloroform. The solubility of this cocrystal and pure salicylic acid were determined by a gravimetric method described previously.<sup>29</sup> Solid liquid mixtures were prepared in tubes with magnetic stir bars. All the material was weighted by a METTLER AE 240 with resolution of 10<sup>-5</sup> g. For comparison with the theophylline – oxalic acid system also the solubility of oxalic acid in acetonitrile has been determined. As reported previously, it is difficult to determine the solubility of oxalic acid by a gravimetric or UV-vis method.<sup>29</sup> For the purpose of the present work, a very precise value is not required, and hence an approximate value of the oxalic acid solubility in acetonitrile at 30 °C was determined by adding solvent to a known amount of solid oxalic acid until it completely dissolved. The solvent was added drop by drop with a syringe, under agitation by a magnetic stir bar until the solution just became clear. The amount of the solution was calculated from the weight change of the syringe.

The invariant points in the cocrystal phase diagram were determined by equilibrating solutions with various mixtures of the two cocrystal components, and analysing both the solution phase and the solid phase. As shown in Figure 2, when the system is in equilibrium and the solid material includes both cocrystal and one of the cocrystal components, the composition of the solution corresponds to the invariant point I1 or I2. In this work, the cocrystal together with one of the cocrystal components was added into acetonitrile to form slurries. Magnetic stir bars were applied with the speed of 400 rpm for at least 12 h at 30 °C to reach equilibrium. Then the slurry was filtered to separate the solid material from the saturated solution. The solid material was examined by XRD and DSC. The saturated solution was divided into two parts: one was used to determine the ratio of solute to solvent by a gravimetric method, and the other one was diluted by pure solvent and analysed by UV-vis. In the UV-vis, the UV absorbance around 270 nm is due to theophylline and that around 300 nm to salicylic acid. Unfortunately, the response from theophylline is somewhat overlapping the salicylic acid peak at 300 nm. Hence, the calibration and measurement for salicylic acid was taken at 310 nm, at which the absorbance was linearly proportional to the salicylic acid concentration. The concentration of theophylline was then calculated from the total amount of the solute in the solution determined by the gravimetric method and the spectroscopically determined salicylic acid concentration.

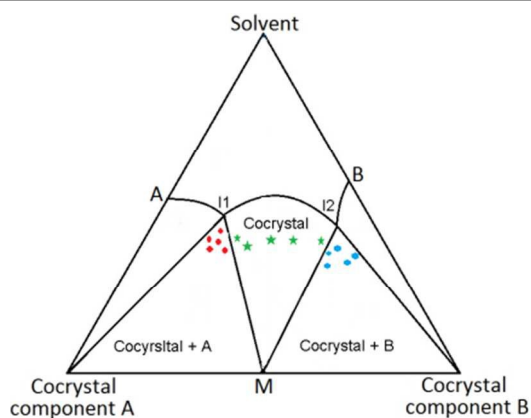


Figure 2 A schematic phase diagram. Red dots: mixture of cocryystals and A crystals; green dots: pure cocryystals; blue dots: mixture of cocryystals and B crystals

The ternary phase diagram of theophylline – oxalic acid in acetonitrile was investigated by analyzing the solid phase of slurries with different composition. Solid material of the cocryystal and one of the cocryystal components were weighted out for the solid phase mixtures with different mole ratio of theophylline to oxalic acid. The ratio was varied from 0.1 to 0.9. Then a small amount of acetonitrile was added to these mixtures to form slurries. These slurries were agitated by magnetic bars with a speed of 400 rpm at 30 °C for at least 48 hours. Then the slurries were filtered and the solid phases were collected and analyzed by XRD and DSC. An approximate cocryystal region was identified by the slurries containing pure cocryystal as the only remaining solid phase, as indicated by the green dots in Figure 2.

### Slurry conversion cocryystalization

Slurry conversion cocryystalization of theophylline – salicylic acid cocryystals was carried out in acetonitrile based on the ternary phase diagram at 30 °C. A solution of theophylline II and salicylic acid in acetonitrile was prepared with a composition close to the solution-cocryystal equilibrium curve I1-I2 (Figure 2). As shown later this solution has a lower concentration of theophylline compared to that of salicylic acid. Then a mixture of 1:1 molar ratio of solid theophylline and solid salicylic acid was added by which the overall mixture composition moves into the “cocryystal region” I1-I2-M, and the conditions for cocryystal formation by slurry conversion were obtained. The slurry was agitated for 5 hours and the solid phase was sampled for DSC analysis.

## Result

### Solid phase characterization

The theophylline – salicylic acid cocryystals obtained from slow evaporation are shown in Figure 3. They are needle-like crystals with a hexagonal cross-section. Figure 4 shows the XRD pattern of the solid phases in this cocryystal system at room temperature and the calculated pattern of the cocryystal using the single crystal structure data in the Cambridge

Structure Database (CSD) – reference KIGLES. The cocryystal XRD pattern is distinctly different from the patterns of pure salicylic acid and the two low temperature forms of pure theophylline. Our single crystal structure analysis derived from the 180 K data shows that the compound cocrytallized in  $P2_1/n$ , with the unit cell of  $a=6.9599$  Å,  $b=25.9822$  Å,  $c=8.0100$  Å,  $\beta=105.224^\circ$ , other information in detail is in Table 1. This corresponds to the CSD data but the unit cell and the beta angle are slightly larger in our data. Each unit cell contains four theophylline and four salicylic acid molecules. Along the  $a$  axis the structure involves  $\pi$ - $\pi$  stacking in a zig-zag fashion as shown in Figure 5, with the distance from the salicylic acid ring centre to its neighbouring two theophylline ring centres being 3.388 Å and 3.857 Å, respectively. An interesting overall feature of the structure is that both component molecules form homopairs of centro symmetric dimers. Alternating dimers are bonded together by a hydrogen bond from the hydrogen of the salicylic acid carboxy group to the basic nitrogen of the theophylline 5-ring all essentially arranged in the  $b$ - $c$  plane as shown in Figure 5. The hydrogen bonding parameters of this cocryystal are listed in Table 2.

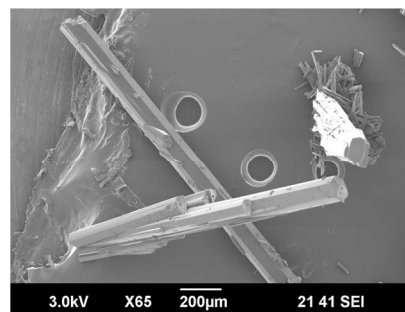


Figure 3 SEM image of theophylline – salicylic acid cocryystals obtained by slow evaporation.

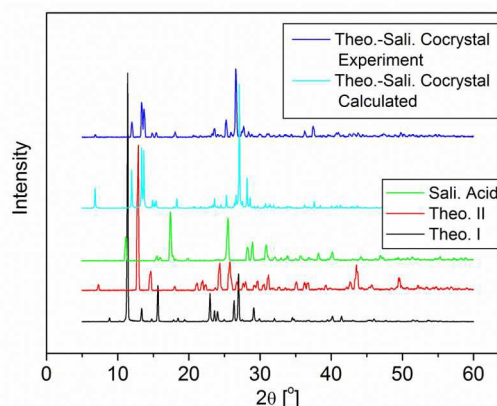


Figure 4 Experimental and calculated powder XRD pattern of theophylline-salicylic acid cocryystal.

When carefully examining the experimental PXRD pattern, it does neither agree with the pattern calculated from the structure determined at 100 K (ref: KIGLES) nor from our own structure determined at 180 K. The unit cell data collected at room temperature from the PXRD shows a structure in  $P2_1/n$ , with

the unit cell of  $a=7.057193 \text{ \AA}$ ,  $b=26.085126 \text{ \AA}$ ,  $c=8.098074 \text{ \AA}$ ,  $\beta=106.2533^\circ$ , which is slightly larger than the structure at 180 K and 100 K. Apparently the cocrystal swells with rising temperature. As shown in Figure 4, the dominating peak from the PXRD pattern of the cocrystal at room temperature is shifted to slightly lower angle compared to that calculated from the structure determined at 180 K. This peak reflects the plane (2 2 -1), which is perpendicular to the direction of  $\pi$ - $\pi$  stacking of the molecules in this crystal, Figure 5. The  $\pi$ - $\pi$  stacking force becomes weaker at increasing temperature, leading to an expansion of the unit cell.

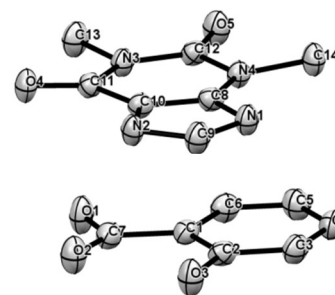
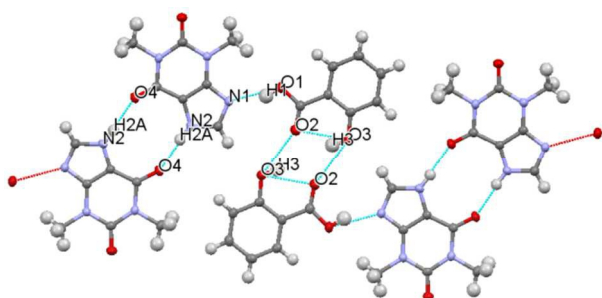
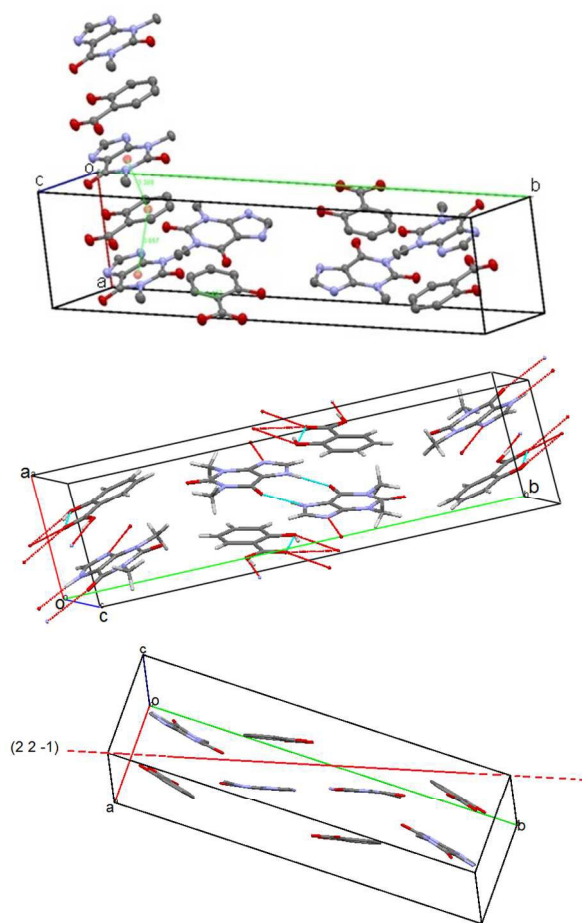


Figure 5 The crystal structure of the theophylline – salicylic acid cocrystal. The Oak Ridge Thermal Ellipsoid Plot (ORTEP) shows the thermal ellipsoids at 50% probability level and H atoms are omitted for clarity.

Table 1 Crystal structure data and structure refinement for the 1:1 theophylline – salicylic acid cocrystal

Empirical formula	$C_{14}H_{14}N_4O_5$
Formula weight	318.29
Temperature/K	180(2)
Crystal system	Monoclinic
Space group	$P2_1/n$
$a/\text{\AA}$	6.9599(5)
$b/\text{\AA}$	25.9822(13)
$c/\text{\AA}$	8.0100(5)
$\alpha/^\circ$	90.00
$\beta/^\circ$	105.224(7)
$\gamma/^\circ$	90.00
Volume/ $\text{\AA}^3$	1397.64(15)
Z	4
$\rho_{\text{calc}}/\text{g/cm}^3$	1.513
$\mu/\text{mm}^{-1}$	0.996
F(000)	664.0
Crystal size/ $\text{mm}^3$	$0.21 \times 0.15 \times 0.12$
Radiation	CuK $\alpha$ ( $\lambda = 1.54178$ )
$2\theta$ range for data collection/ $^\circ$	11.94 to 133.18
Index ranges	$-7 \leq h \leq 8, -28 \leq k \leq 30, -7 \leq l \leq 9$
Reflections collected	4694
Independent reflections	2472 [ $R_{\text{int}} = 0.0395$ ]
Data/restraints/parameters	2472/0/234
Goodness-of-fit on $F^2$	1.066
Final R indexes [ $I \geq 2\sigma(I)$ ]	$R_1 = 0.0718, wR_2 = 0.1994$
Final R indexes [all data]	$R_1 = 0.0886, wR_2 = 0.2085$
Largest diff. peak/hole / $e \text{ \AA}^{-3}$	0.42/-0.39

Table 2 The hydrogen bond interaction in the 1:1 theophylline – salicylic acid cocrystal

Hydrogen bond	D-H ( $\text{\AA}$ )	H...A ( $\text{\AA}$ )	D...A ( $\text{\AA}$ )	$\angle\text{DHA}$ ( $^\circ$ )
$O_1-H_1 \cdots N_1$	0.86	1.86	2.67	158
$N_2-H_{2A} \cdots O_4$	0.88	1.92	2.79	175
$O_3-H_3 \cdots O_2^{\#1}$	0.84	2.25	2.87	131
$O_3-H_3 \cdots O_2^{\#2}$	0.84	1.96	2.65	139

#1 Intermolecular hydrogen bond, symmetry code:  $-x, -y, -z$ ; #2 Intramolecular hydrogen bond, symmetry code:  $x, y, z$ ; the atom numbers are shown in the second picture in Figure 5.

Figure 6 shows the DSC curve of the theophylline – salicylic acid cocrystal, and the pure cocrystal components for comparison. The melting temperature of this cocrystal is at  $188.5 \text{ }^\circ\text{C}$  (onset), in between of the melting points of the cocrystal components.

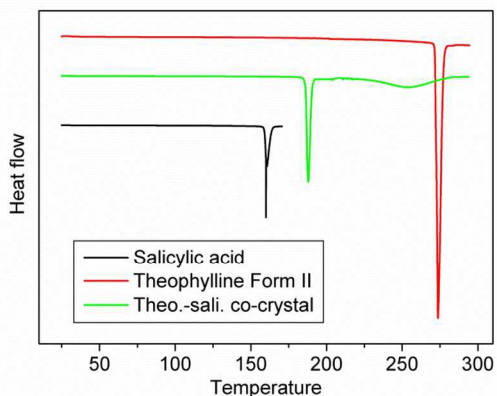


Figure 6 The DSC result of theophylline – salicylic acid cocrystal and pure cocrystal components.

### Solubility and phase diagram

The theophylline – salicylic acid cocrystal dissolves congruently in chloroform. At 30 °C, the solubility of the pure cocrystal in chloroform determined to 0.040 mol/L, while the corresponding value for pure theophylline Form II is 0.045 mol/L,<sup>12</sup> and for pure salicylic acid is 0.253 mol/L.<sup>34</sup> As can be deduced from our previous analysis,<sup>29</sup> the Gibbs free energy of formation of the cocrystal from the pure solid components can be calculated as:

$$\Delta G_{form} = -RT \ln \frac{a_{liq}^{A,+} a_{liq}^{B,+}}{a_{liq}^A a_{liq}^B} \quad (1)$$

In the numerator, the  $a_{liq}^{A,+}$  and  $a_{liq}^{B,+}$  are the activities of the solute in a solution in equilibrium with either of the pure cocrystal components, respectively. In the denominator, the  $a_{liq}^A$  and  $a_{liq}^B$  are the activity of the cocrystal components in a solution in equilibrium with the pure cocrystal. If activities can be approximated by mole fractions, the free energy of cocrystal formation from the metastable theophylline II and salicylic acid receives a value of -4.918 kJ/mol cocrystal at 30 °C. The cocrystal is thermodynamically more stable than a stoichiometric mechanical mixture of the pure cocrystal components.

The theophylline – salicylic acid cocrystal dissolves incongruently in methanol, ethanol, and acetonitrile as can be deduced from simple dissolution experiments where the solid cocrystal transforms into the solid pure components. Equilibrium data for the theophylline/salicylic acid/acetonitrile are given in Table 3 and the phase diagram is shown in Figure 7. The anticipated solid phase mixture at the invariant points is verified by the XRD spectra in Figure 8. In Figure 8(a), the black curve shows peaks from both the cocrystal and theophylline II, revealing that the slurry contains both solid phases, and accordingly the solution represents the invariant point of the region of “cocrystal and theophylline II” in the ternary phase diagram. Similarly Figure 8(b) verifies the solid

phase mixture at the invariant point of “cocrystal and salicylic acid”.

Table 3 Equilibrium Solution Compositions of Various Solid Phases in Acetonitrile at 30 °C

Composition of solid phases	Mole fraction		
	Theophylline	Salicylic acid	Acetonitrile
<i>Theophylline II</i>	0.00054	0	0.99946
Theo. II &	0.00118	0.00235	0.99647
Cocrystal (E1)*	0.00128	0.00259	0.99614
Cocrystal &	0.01023	0.02504	0.96473
Sali. acid (E2)	0.01015	0.02600	0.96385
Salicylic acid <sup>25</sup>	0	0.03443	0.96557

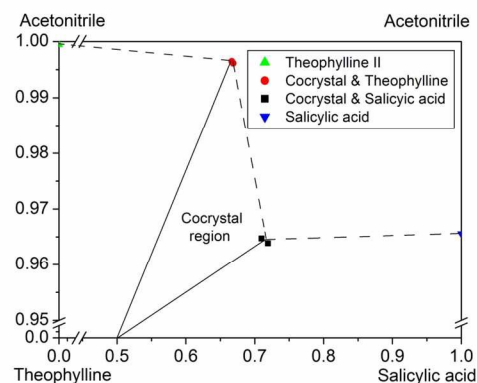


Figure 7 Experimental determinations of the invariant points in the ternary phase diagram of theophylline/salicylic acid/acetonitrile.

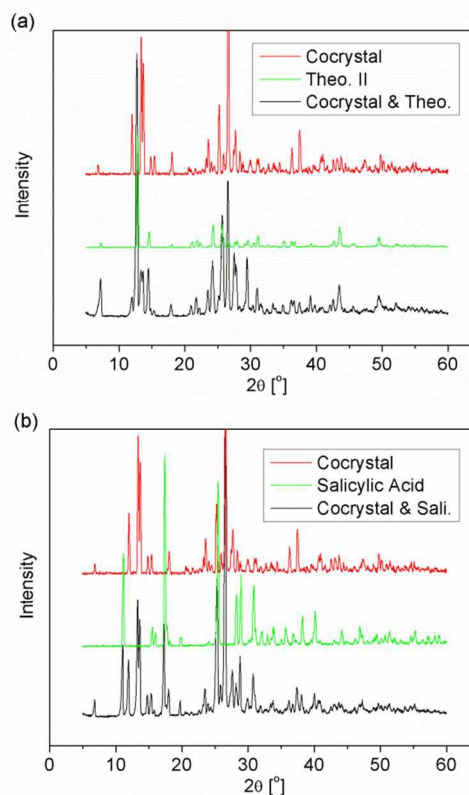


Figure 8 Comparison of invariant point solid phases from acetonitrile with pure compound XRD spectra.

The theophylline – oxalic acid cocrystal dissolves congruently in chloroform as shown previously but also in acetonitrile as shown in Figure 9.<sup>29</sup> The red dots present the overall composition starting point that will lead to the status of pure cocrystal solid phase in equilibrium with the solution. The points in blue and argenta reveal starting points that will lead to a solid phase mixture of the cocrystal together with theophylline and salicylic acid, respectively, in equilibrium with the solution.

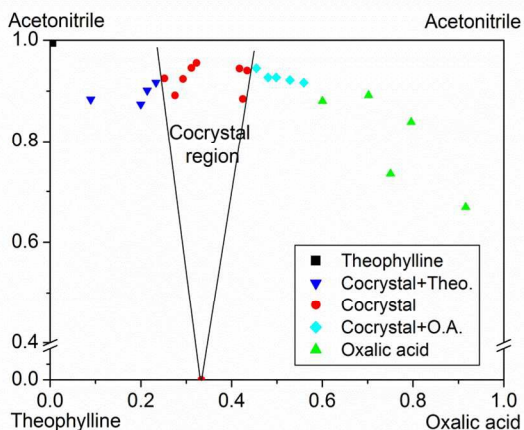


Figure 9 A phase diagram of the theophylline/oxalic acid/acetonitrile system.

### Slurry conversion cocrystallization

The starting point for the slurry conversion is a 1:1 physical mixture of the two pure solid components and a solution, the whole system having an overall composition inside the cocrystal region. As the cocrystal starts to form stoichiometric amounts of the pure components are consumed. Along the slurry conversion the overall composition of the system remains the same and accordingly remains in the cocrystal region, and

when all pure solid material has transformed the system is a mixture of pure cocrystal material and a corresponding saturated solution. Adding further 1:1 molar ratio of solid theophylline and solid salicylic acid brings the system overall just closer to the pure cocrystal composition point without moving out of the cocrystal region. The DSC analysis of the solid phase from slurry conversion crystallization experiments shows the cocrystal peak only, which shows that the solid phase is the pure theophylline – salicylic acid cocrystal and verifies that the mixture is in the cocrystal region of the phase diagram. Obviously, slurry conversion is a feasible method of producing the cocrystal. The previously reported slurry conversion cocrystallization of the theophylline – glutaric acid cocrystal,<sup>12</sup> is another example to illustrate that a cocrystal can be successfully prepared by slurry conversion crystallization also for incongruently dissolving cocrystals as long as the process is operated in a slurry with an overall composition within the “cocrystal region” in the ternary phase diagram.

### Discussion

The melting temperatures and the free energy of formation of the three theophylline cocrystals are given in Table 4 together with information over the crystal structures.

The melting/decomposition temperature of the three theophylline cocrystals and their cocrystal components are presented in Figure 10. In all these three cases, the melting/decomposition temperature of cocrystal is between the melting temperature of the pure cocrystal components, and increases with increasing melting temperature of the cofomer. Also shown in Table 4, is that the Gibbs free energy of formation of these cocrystals also increases (the cocrystal becomes more stable in relation to its components) with increasing melting point of the cofomer.

Table 4 Crystal structure information of cocrystal and melting/decomposition point, density\*,  $\Delta H_{melting}$ ,  $\Delta G_{form}$ ,  $\Delta H_{form}$ ,  $\Delta S_{form}$

Cocrystal	Volume of unit cell	Volume of conformer	N <sub>theo</sub>	N <sub>acid</sub>	Packing coefficient	Melting temp. of conformer (peak value)	Melting/decomp. temp. of cocrystal	$\Delta H_{melting}$ [kJ/mol]	$\Delta G_{form}$ [kJ/mol] (30 °C)	$\Delta H_{form}$ [kJ/mol] (30 °C)	$\Delta S_{form}$ [kJ/mol·K] (30 °C)
Theo.-O.A.	934.06	65.48	4	2	0.752	189	230 (peak value)	--	-5.62	--	--
Theo.-Sali.	1382.32	116.37	4	4	0.750	159	188.5	46.37	-4.92	87.63	0.305
Theo.-Glu.	2785.74	113.8	8	8	0.737	99	119.5	32.91	-0.39	30.73	0.103

\* the unit cell volume of theophylline is 142.79 Å<sup>3</sup>.

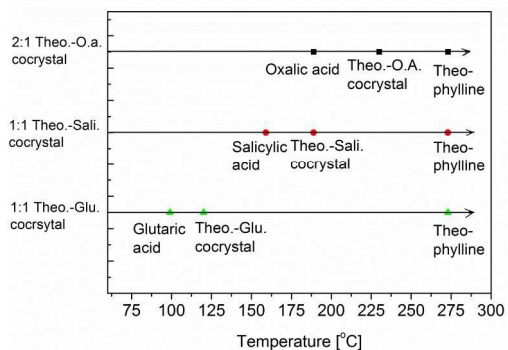


Figure 10 The melting/decomposition points of theophylline cocrystals and their cocrystal components.

Figure 11 shows the standard DSC curves comparing the behaviour of the theophylline cocrystal with salicylic acid and glutaric acid respectively, with that of the corresponding 1 : 1 mechanical mixture of the components. The two lower diagrams show how the system enthalpy changes with the temperature using the melt at 290 °C as reference. These graphs are obtained by integration of the standard DSC data after necessary unit conversions. In Figure 11 (a), the 1:1 molar ratio mechanical mixture curve of theophylline/salicylic acid has an endothermic peak approximately at the melting point of salicylic acid. This peak is directly followed by a smaller exothermic peak likely to describe the formation of the cocrystal since it is followed in turn by a clear melting peak at the melting temperature of the cocrystal. However, at increasing temperature, there is an unknown endothermic peak at 244°C, which may indicate the existence of a new solid phase, either a new cocrystal or cocrystal polymorph or an unknown form of theophylline. The final peak corresponds to the melting of theophylline. The corresponding DSC graph for the theophylline-glutaric acid system is different. The theophylline – glutaric acid cocrystal melts at 119.5 °C. The mechanical mixture of pure 1:1 molar ratio theophylline/glutaric acid has a first peak at 75 °C corresponding to the polymorphic transformation of glutaric acid, and followed by a peak at the melting point of glutaric acid at 99 °C. There is only a tiny trace of the cocrystal peak and there is no “unknown” peak at higher temperature. Comparing the relative enthalpies of the cocrystal and its 1:1 mechanical mixture, the difference is the enthalpy of formation of the cocrystal. At 30 °C this value estimates to 275.32 J/g for the theophylline – salicylic acid cocrystal, and to 98.42 J/g for the theophylline –glutaric acid cocrystal, corresponding to 87.63 kJ/mol and 30.73 kJ/mol, respectively. From the free energy and enthalpy of cocrystal formation the entropy of formation is calculated to 0.305 kJ/mol·K for the theophylline – salicylic acid cocrystal, and to 0.103 kJ/mol·K for the theophylline – glutaric acid cocrystal at 30 °C. Accordingly, in both cases the cocrystal formation is an endothermic process, but the increase in entropy leads to a favourable reduction in free energy.

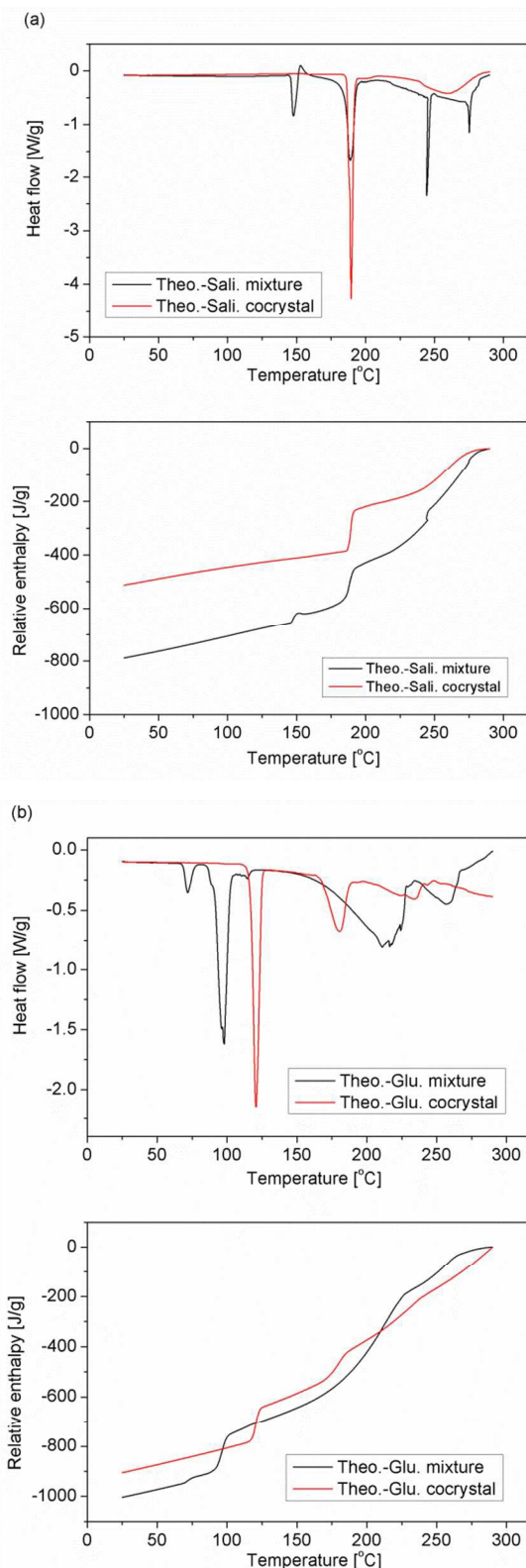


Figure 11 (a) The standard DSC curve and relative enthalpy of theophylline – salicylic acid cocrystal and its 1:1 coformer mixture. (b) The standard DSC curve and relative enthalpy of theophylline – glutaric acid cocrystal and its 1:1 coformer mixture.

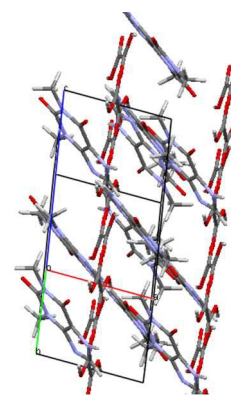
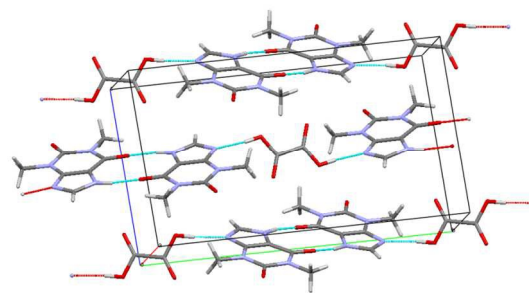
The cocrystals of theophylline with oxalic acid, glutaric acid and salicylic acid all share different features in their crystal structures. In all these three cases, theophylline and the cofomers are connected via the best H-bond acceptor of theophylline (the basic N), and the best H-bond donor of the cofomer (the hydroxyl H) (Figure 13). This complies with the general trends for cocrystal formation, because the system tends to maximize electrostatic interaction.<sup>35</sup> Secondly, in all these three cocrystals, theophylline molecules connect to each other by the carbonyl oxygen and the secondary amine hydrogen, to form theophylline dimers. Another interesting point is that in the salicylic acid cocrystal both components are engaged in homo dimerization, while for oxalic acid and glutaric acid cocrystals the cofomer does not appear as dimers.

The volume of the unit cell and the number of molecules in each unit cell in Table 4 are obtained by using the Mercury software and the single crystal structure data.<sup>1,36</sup> The volume of each molecule was calculated by Material Studio using the Van de Waals radii and the geometry of the molecule as it is in the cocrystal structure. The packing coefficient can be calculated as:

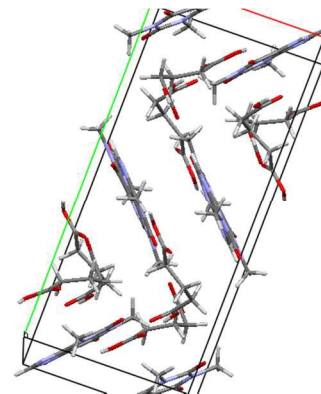
$$K_p = (nV_{theo.} + mV_{acid.})/V_{cell}$$

where  $V_{theo.}$  is the molecular volume of theophylline,  $n$  the number of theophylline molecules,  $V_{acid.}$  is the molecular volume of the cofomer,  $m$  the number of cofomer molecules in the unit cell, and  $V_{cell}$  is the volume of the cocrystal unit cell. The data in Table 5 show the melting/decomposition point of different theophylline cocrystals increases from 120 °C to 230 °C with increasing packing coefficient from 0.737 to 0.752.

The packing coefficient is affected by the bonding strength between the molecules – van der Waals forces, hydrogen bonding and other electrostatic forces as well as by the geometry of the molecules. The theophylline molecule has most of its atoms in the same plane. The oxalic acid molecule is fairly small (Table 5), and each oxalic acid molecule connects with two theophylline dimers, like a small chain link connecting two flake fragments. This leads to relatively high packing efficiency (as shown in Figure 12(a)). The molecular volume of salicylic acid and glutaric acid is roughly the same. The shape of the salicylic acid molecule is more flat, having most of its atoms in the same plane, while the overall shape of the glutaric acid molecule is fairly symmetrical, though slightly longer in one dimension. So the theophylline – salicylic acid cocrystal has a rather layered structure (Figure 5), while the theophylline – glutaric acid cocrystal does not (Figure 12(b)). Therefore the theophylline – glutaric acid cocrystal has much larger unit cell volume, and the lowest packing efficiency.



(a) theophylline – oxalic acid cocrystal



(b) theophylline – glutaric acid cocrystal

Figure 12 The crystal structure of the theophylline – oxalic acid and theophylline – glutaric acid cocrystals

Table 5 lists the mole fraction solubility of the pure cocrystal components in various solvents, the ratio of their mole fraction solubility to that of theophylline, and the dissolution behaviour (congruent/incongruent) of the cocrystal. The theophylline – salicylic acid cocrystal dissolves congruently in chloroform. In acetonitrile, the solubility of theophylline is approximately 15% of that in chloroform, while the solubility of salicylic acid is about 80% higher, and accordingly the solubility mole fraction ratio is twelve times higher and the cocrystal dissolves incongruently, as is illustrated in Figure 13 a). For theophylline – glutaric acid the situation is much the same. With respect to the metastable form of theophylline, the system is congruent in chloroform but incongruent in acetonitrile where the solubility ratio is in the order of 50 times higher. Interestingly, with

respect to the stable form of theophylline, the glutaric acid cocrystal dissolves incongruently in chloroform<sup>12</sup> as is shown in Figure 13(b). The theophylline – oxalic acid cocrystal dissolves congruently in both chloroform/methanol and in acetonitrile.

The schematic phase diagrams for the three cocrystal systems are shown in Figure 13. In all the three cases, the cocrystal region (where the cocrystal is stable) shifts towards the cofomer side of the diagram with increasing ratio of the mole fraction solubilities. The solubility ratio of glutaric acid to theophylline increases in order for “glu./theo. I in chloroform” (a), “glu./theo. II in chloroform” (b), “glu./theo. I in acetonitrile” (c), and “glu./theo. II in acetonitrile” (d). Correspondingly the cocrystal region shifts more and more towards the cofomer side in the same order, Figure 13(a). For the theophylline – salicylic acid cocrystal systems, when the mole fraction solubility ratio increases, from 5.5 of “sali./theo. II in chloroform” (e) to 63 of “sali./theo. II in acetonitrile” (f), the cocrystal region clearly shifts towards the cofomer side, as

shown in Figure 13(b). In addition, even for the theophylline – oxalic acid cocrystal systems, from the approximately determined ternary phase diagram in acetonitrile, it can be observed that when the mole fraction solubility ratio increases from unity to about 100, the invariant point corresponding to the composition of the solution in equilibrium with “theophylline & cocrystal” moves from theophylline side (theo./(theo.+o.a.)  $\approx$  0.9) (g) towards the stoichiometric cocrystal line (theo./(theo.+o.a.)  $\approx$  0.74) (h) (Figure 13(c)). As only half of the cocrystal region is determined for theophylline/oxalic acid/chloroform system, the undetermined part is indicated by dashed lines. Accordingly for the same cocrystal system there appears to be a trend that can be rationalised by the theophylline/coformer solubility ratio over different solvents. However, by comparing the results from the three different systems the solubility ratio cannot be safely used across different cofomers.

Table 5 Mole fraction solubility of cocrystal components and the dissolution property of cocrystals in various solvents

System	Mole fraction of pure theophylline solubility	Mole fraction of pure cofomer solubility	[Cofomer]/[Theo.]	Dissolution behaviour of cocrystal
Theo. I/Glutaric acid/Chloroform [a]	0.003167	0.010355	3.269	Incongruent
Theo. II/Glutaric acid/Chloroform [b]	0.003614	0.010355	2.865	Congruent
Theo. I/Glutaric acid/Acetonitrile [c]	0.00038	0.05431	142.92	Incongruent
Theo. II/Glutaric acid/Acetonitrile [d]	0.00054	0.05431	100.57	Incongruent
Theo. II/Salicylic acid/Chloroform [e]	0.003614	0.019977	5.528	Congruent
Theo. II/Salicylic acid/Acetonitrile [f]	0.00054	0.034113	63.172	Incongruent
Theo. II/Oxalic acid/(Chloroform/methanol) [g]	0.02056	0.02128	1.035	Congruent
Theo. II/Oxalic acid/Acetonitrile [h]	0.00054	ca. 0.05519	ca. 100	Congruent

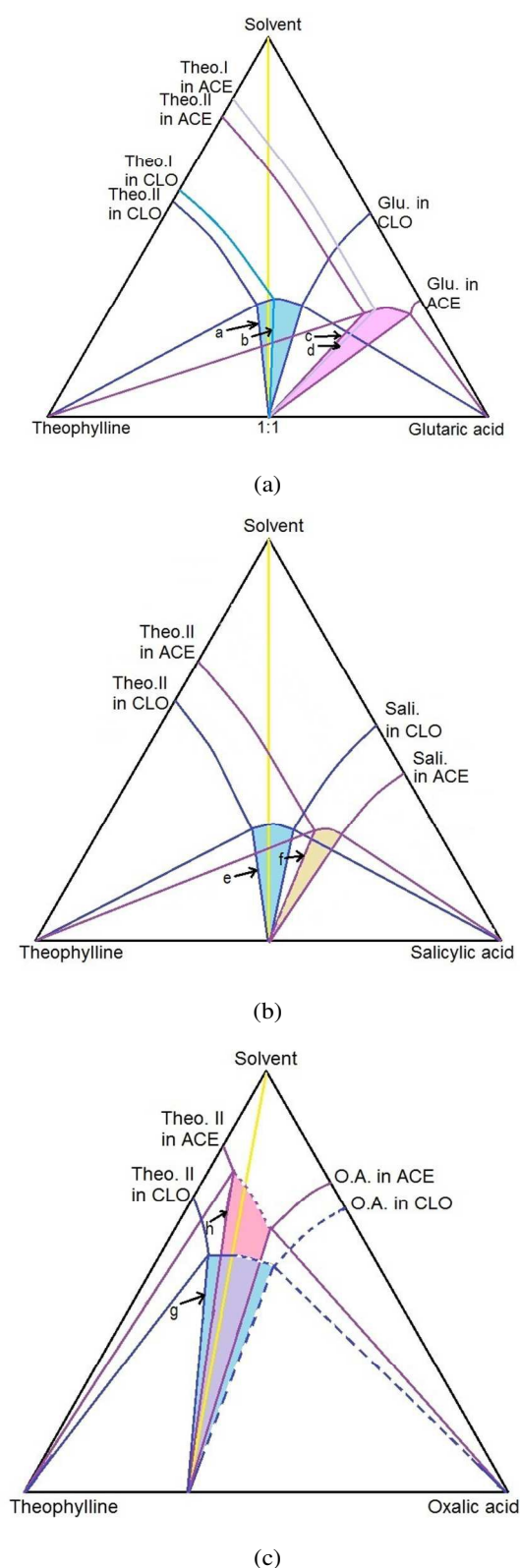


Figure 13 (a) The schematic phase diagram of theophylline – glutaric acid cocrystals. (b) The schematic phase diagram of theophylline – salicylic acid cocrystals. (c) The schematic phase diagram of theophylline – oxalic acid cocrystals. Abbreviations: ACE – acetonitrile, CLO – chloroform.

The ternary phase diagram of the cocrystal systems is important in the design of the manufacturing process of cocrystals. All three theophylline cocrystals have been successfully produced by slurry conversion crystallization. These crystallizations verify that, with access to the ternary phase diagram, cocrystals can be readily produced by slurry conversion crystallization, regardless of if the dissolution is congruent or not, as long as the operation is carried out within the region of the phase diagram where the cocrystal is stable or have sufficient metastability.

## Conclusions

The free energy of formation of the theophylline-salicylic acid cocrystal from its pure components amounts to  $-4.92$  kJ/mol, and the cocrystal melting point is  $188.5$  °C. The cocrystal dissolves congruently in chloroform but incongruently in acetonitrile, methanol and ethanol. However, the cocrystal can be produced by slurry conversion in acetonitrile by preparing a mixture of the two components that corresponds to the region where the cocrystal is stable, and then adding further solid material of the pure compounds in stoichiometric amounts.

The properties of the theophylline – salicylic acid cocrystal have a lot in common with the theophylline – oxalic acid cocrystal and the theophylline – glutaric acid cocrystal. In terms of structure, all the three cocrystals of theophylline are connected by  $N\cdots H$  hydrogen bonds between the basic N atom, the best hydrogen bond acceptor of theophylline, and the hydroxyl H atom, the best hydrogen bond donor of the coformer. Theophylline molecules form homo-dimers in all these cocrystal structures, and in all three systems, the cocrystal melting/decomposition point is between the melting point of theophylline and the coformer. The melting point of the theophylline cocrystal increases from  $120$  °C to around  $230$  °C with increasing melting temperature of the coformer, and the packing efficiency of the cocrystal increases similarly. All three cocrystals have a negative Gibbs free energy of formation,  $\Delta G_{\text{form}}$ , the value of which increases with increasing with increasing coformer melting point.

For the same cocrystal, the cocrystal region in the ternary phase diagram shifts towards the coformer side with increasing solubility ratio of the coformer to theophylline. However, this relation for a particular cocrystal system in different solvents cannot be safely extended across systems of different coformers.

## Acknowledgements

The authors appreciate and acknowledge the Swedish Research Council for financial support (621-2007-3982), and Rasmuson the support of the Science Foundation Ireland to the Synthesis and the Solid State Pharmaceutical Centre, SSPC. Thanks to Zhengbao Yu and Junliang Sun at College of Chemistry and Molecular Engineering, Peking University for collecting the single crystal X-ray diffraction data.

## Notes and references

<sup>a</sup> Department of Chemical Engineering and Technology, Royal Institute of Technology (KTH), Stockholm, Sweden. E-mail: shuoz@kth.se.

<sup>b</sup> Department of Chemical and Environmental Science, Materials and Surface Science Institute, Synthesis and Solid State Pharmaceutical

Center, University of Limerick, Limerick, Ireland. E-mail: rasmuson@ket.kth.se; ake.rasmuson@ul.ie.

<sup>c</sup> Department of Materials and Environmental Chemistry, Stockholm University, SE-106 91 Stockholm, Sweden. Email: [hong.chen@mmk.su.se](mailto:hong.chen@mmk.su.se).

<sup>d</sup> Faculty of Material Science and Chemistry, China University of Geosciences, 430074 Wuhan, China.

- 1 A. V. Trask, W. D. S. Motherwell and W. Jones, *Int. J. of Pharm.*, 2006, **320**, 114.
- 2 A. V. Trask, W. D. S. Motherwell, W. Jones, *Cryst. Growth Des.*, 2005, **5**, 1013.
- 3 S. Karki, T. Frišćić, W. Jones and W. D. S. Motherwell, *Mol. Pharm.*, 2007, **4**, 347.
- 4 T. Frisci, L. Fabian, J. C. Burley, D. G. Reid, M. J. Duer and W. Jones, *Chem. Commun.*, 2008, **14**, 1644.
- 5 A. M. Chen, M. E. Ellison, A. Peresykin, R. M. Wenslow, N. Variankaval, C. G. Savarin, T. K. Natishan, D. J. Mathre, P. G. Dormer, D. H. Euler, R. G. Ball, Z. Ye, Y. Wang and I. Santos, *Chemical Communications*, 2007, **4**, 419.
- 6 D. P. McNamara, S. L. Childs, J. Giordano, A. Iarriccio, J. Cassidy, M. S. Shet, R. Mannion, E. O'Donnell and A. Park, *Pharm. Res.*, 2006, **23**, 1888.
- 7 M. B. Hickey, M. L. Peterson, L. A. Scoppettuolo, S. L. Morrisette, A. Vetter, H. Guzman, J. F. Remenar, Z. Zhang, M. D. Tewa, S. Haley, M. J. Zaworotko and Ö. Almarsson, *Eur. J. Pharm. Biopharm.*, 2007, **1**, 112.
- 8 N. Schultheiss and A. Newman, *Cryst. Growth Des.*, 2009, **9**, 2950.
- 9 R. D. Bailey Walsh, M. W. Bradner, S. Fleischman, L. A. Morales, B. Moulton, N. Rodriguez-Horedó, M. J. Zaworotko, *Chem. Commun.*, 2003, **2**, 186.
- 10 A. D. Bond, *CrystEngComm.*, 2006, **8**, 333.
- 11 R. A. Chiarella, R. J. Davey and M. L. Peterson, *Cryst. Growth Des.*, 2007, **7**, 1223.
- 12 S. Zhang and Å. C. Rasmuson, *Cryst. Growth Des.*, 2013, **13**, 1153.
- 13 A. Ainouz, J. R. Authelin, P. Billot and H. Lieberman, *Int. J. Pharm.*, 2009, **374**, 82.
- 14 Z. Q. Yu, P. S. Chow and R. B. H. Tan, *Cryst. Growth Des.*, 2010, **10**, 2382.
- 15 E. Gagniere, D. Mangin, F. Puel, J. Valour, J. P. Klein and O. Monnier, *J. Cryst. Growth.*, 2011, **316**, 118.
- 16 E. Gagniere, D. Mangin, F. Puel, C. Bebon, J. P. Klein, O. Monnier and E. Garcia, *Cryst. Growth Des.*, 2009, **9**, 3376.
- 17 E. Gagniere, D. Mangin, F. Puel, A. Rivoire, O. Monnier, E. Garcia and J. P. Klein, *J. Cryst. Growth*, 2009, **311**, 2689.
- 18 D. M. Croker, R. J. Davey, Å. C. Rasmuson and C. C. Seaton, *Cryst. Growth Des.*, 2013, **13**, 3754.
- 19 T. Leyssens, G. Springuel, R. Montis, N. Candoni and S. Veessler, *Cryst. Growth Des.*, 2012, **12**, 1520.
- 20 E. Suzuki, K. Shimomura, K. Sekiguchi, *Chem. Pharm. Bull.*, 1989, **37**, 493.
- 21 D. Khamar, I. J. Bradshaw, G. A. Hutcheon, L. Seton, *Cryst. Growth Des.*, 2012, **12**, 109.
- 22 Phadnis V. N.; Suryanarayanan R. J. *Pharm. Sci.*, 1997, **86**, 1256.
- 23 C. Nunes, A. Mahendrasingam and R. Suryanarayanan, *Pharm. Res.*, 2006, **23**, 2393.
- 24 K. Matsuo and M. Matsuoka, *Cryst. Growth Des.*, 2007, **7**, 411.
- 25 L. Seton, D. Khamar, I. J. Bradshaw and G. A. Hutcheon, *Cryst. Growth Des.*, 2010, **10**, 3879.
- 26 Y. Ebisuzaki, P. D. Boyle, J. A. Smith, *Acta Crystallogr., Sect. C: Cryst. Struct. Commun.*, 1997, **53**, 777.
- 27 D. Khamar, R. G. Pritchard, I. J. Bradshaw, G. A. Hutcheon and L. Seton, *Acta Crystallogr., Sect. C: Cryst. Struct. Commun.*, 2011, **C67**, 0496.
- 28 S. Zhang and A. Fischer, *Acta Crystallogr., Sect. E: Struct. Rep. Online*, 2011, **E67**, o3357.
- 29 S. Zhang and Å. C. Rasmuson, *CrystEngComm.*, 2012, **14**, 4644.
- 30 *Crysalis Software System*, Oxford Diffraction Ltd, 2011.
- 31 G. M. Sheldrick, *Acta Cryst. A*, 2008, **64**, 112.
- 32 S.W. Zhang, I. A. Guzei, M. M. de Villiers, L. Yu and J. F. Krzyzaniak, *Cryst. Growth Des.*, 2012, **12**, 4090.
- 33 M. A. Oliveira, M. L. Peterson and R. J. Davey, *Cryst. Growth Des.*, 2011, **11**, 449.
- 34 F. L. Nordström and Å. C. Rasmuson, *J. Chem. Eng. Data.*, 2006, **51**, 1668.
- 35 M. C. Etter, *J. Phys. Chem.*, 1991, **95**, 4601.
- 36 S. L. Childs, G. P. Stahly and A. Park, *Mol. Pharm.*, 2007, **4**, 323.